Research Article

Hamid Reza Ansari and Zoheir Kordrostami*

Design and simulation of a MEMS MIM capacitive pressure sensor with high sensitivity in low pressure range

https://doi.org/10.1515/ehs-2021-0017
Received August 7, 2021; accepted November 6, 2021;
published online November 18, 2021

Abstract: In this paper, the improvement of the sensitivity of a capacitive MEMS pressure sensor is investigated. The proposed spring for the sensor can increase the sensitivity. Silicon is used as the substrate and gold and aluminium nitrate are used as the diaphragm and the dielectric layer, respectively. The dimensions of the diaphragm are 150 μm × 150 μm, which is suspended by four springs. The air gap between the diaphragm and the top electrode is 1.5 μm. The proposed structure is an efficient sensor for the pressures in the range of 1–20 kPa. By using the proposed design, the sensitivity of the MEMS sensor in 18 kPa has improved to 663 ($\times 10^{-3}$ pF/kPa).

Keywords: capacitive sensor; diaphragm; MEMS pressure sensor; MIM; sensitivity.

Introduction

Today, the devices based on the MEMS technology, including switches (Ansari and Taghaddosi 2020; Rebeiz 2003), accelerometers and energy harvesters (Kordrostami and Roohizadegan 2018), have flourished because of the advantages such as the integrability with CMOS. MEMS technology has been welcomed by designers of electronic devices due to its small size and low power consumption (Amiri and Kordrostami 2018; Ansari and Kordrostami 2020; Mafinejad et al. 2015). Also, capacitive pressure sensors based on MEMS technology are economically viable after mass production, so a MEMS sensor may have many enthusiasts in the market. Capacitive pressure sensors are also generalizable with MEMS technology and look very attractive compared to similar models due to the small size and low weight of the sensor (Ansari and Khosroabadi 2018; Ansari, Kordrostami, and Hamedi 2020; Mafinejad et al. 2017; Rao et al. 2020). The operation mechanism of the capacitive sensors is based on the changes in the capacitance between the diaphragm and the substrate that is a function of the pressure. These sensors consist of two parts: movable part (diaphragm) and a fixed part including the upper electrode (metal), the dielectric layer (insulator) and the lower electrode (metal) (MIM). By applying force to the diaphragm and bending it down, capacitive changes occur that lead to a change in sensitivity. The input of the device is force or pressure and its output is capacitive changes (Ghoddus and Kordrostami 2018; Ghoddus, Kordrostami, and Amiri 2019; Rao et al. 2020). The design parameters such as materials used in the sensor, the thickness of the diaphragm and the dielectric layer, the air gap, and the structure dimensions affect the sensitivity considerably (Ansari and Khosroabadi 2019; Kordrostami and Roohizadegan 2019; Mafinejad, Ansari, and Khosroabadi 2020; Rao et al. 2020). Researchers have tried to increase the sensitivity such capacitive sensors by changing the dimensions and materials. However, a more promising approach to increase the sensitivity is to use new designs for the springs attached to the diaphragm. This way, the displacement of the diaphragm can become more sensitive to the pressure changes.

In this paper, a MEMS capacitive pressure sensor is designed and simulated. The proposed new serpentine springs could increase the sensitivity of the sensor. The organization of the paper is as follows: “Design” section describes the sensor design and the displacement changes at different pressures. “Results and discussion” section illustrates explains the spring stiffness coefficient, the amount of capacitance and the sensitivity with the corresponding discussions and in “Conclusion” section, the paper is concluded.

***Corresponding author: Zoheir Kordrostami**, Department of Electrical and Electronics Engineering, Shiraz University of Technology, Shiraz, Iran, E-mail: kordrostami@sutech.ac.ir
Hamid Reza Ansari, Department of Electrical and Electronics Engineering, Shiraz University of Technology, Shiraz, Iran

Design

The MEMS capacitive pressure sensor consists of a fixed part and a movable membrane (diaphragm). By applying the pressure to the surface of the diaphragm, the gap between the diaphragm and the below electrode changes. Figures 1 and 2 show the diaphragm at rest and in the operation mode. As can be seen, the springs have been designed efficiently to provide high sensitivity. The springs have been placed so that the highest sensitivity would be achieved.

Gold and aluminum nitrate have been used as the electrodes and the dielectric layer, respectively. The gap between the diaphragm and the dielectric layer (air gap) is 1.5 μm. A Silicon substrate has been used. The total capacitance is obtained from the sum of two capacitances. The capacitance which has been formed with the dielectric layer (C_1) and the capacitance which is created in the air gap (C_2) and varies with the pressure.

$$C_1 = \frac{\epsilon_0 \epsilon_r A}{d} \tag{1}$$

$$C_2 = \frac{\epsilon_0 A}{h} \tag{2}$$

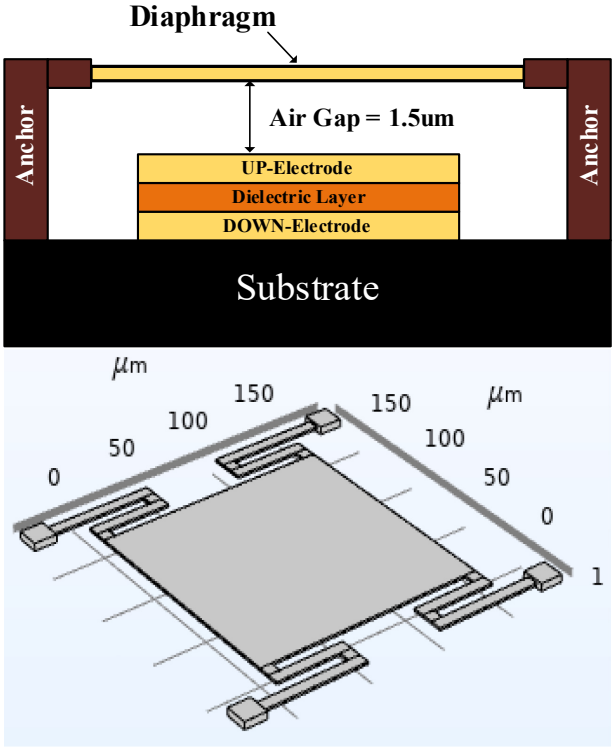

Figure 1: The up state mode (before applying force).

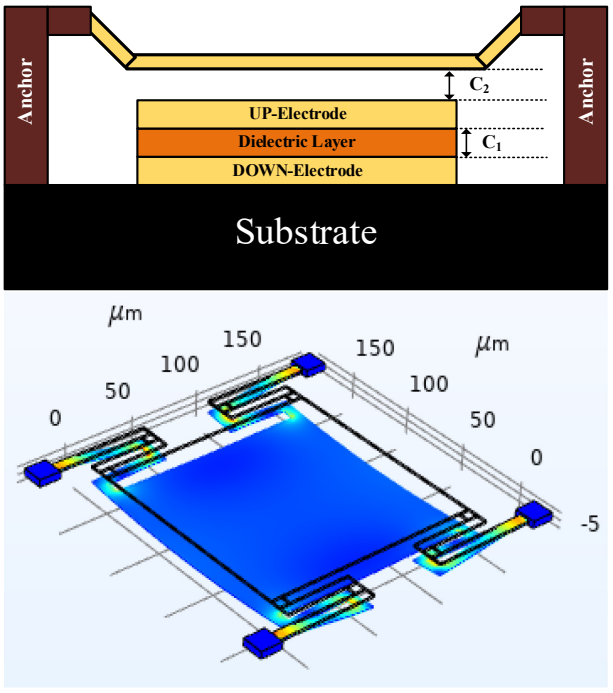

Figure 2: The down state mode (after applying force).

where, d is the dielectric thickness (0.5 μm), h is the air gap, and A is the cross-sectional area of the diaphragm.

The dimensions of the sensor are shown in Figure 3a. The thickness of the diaphragm is equal to 5 μm. Figure 3b shows the displacement of different parts of the sensor after applying a 20 kPa pressure to the diaphragm. Also, the displacement and stress profile of the sensor with the simple spring have been shown in Figure 4.

As can be seen in Figures 3 and 4, by using the proposed springs the displacement of the diaphragm has been increased compared to the simple spring.

In MEMS capacitive sensors, the displacement is expected to increase proportional to the pressure, resulting in an almost linear response. Figure 5 shows the amount of diaphragm displacement versus pressure (linear response). As can be seen, Figure 5 is an uptrend curve that increases the displacement with increasing pressure. According to Figure 5, the maximum pressure applicable to the sensor is 20 kPa. The proposed sensor performance would be linear in the range of 1–20 kPa.

As shown in Figure 5, the response of the proposed sensor has a very good linearity which is a desirable characteristics. Also it has been shown that the displacement of the proposed structure has been increased compared to the simple structure which shows the efficiency of the proposed design.

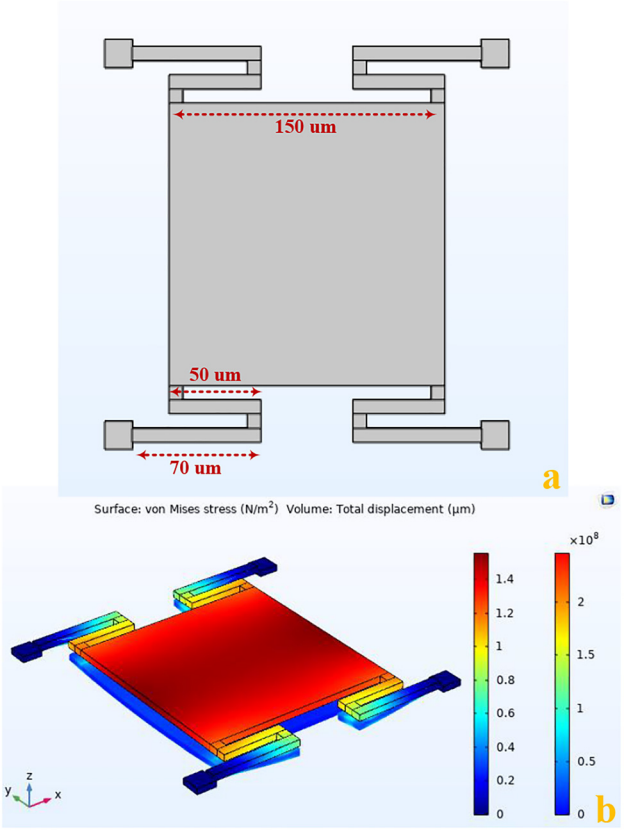

Figure 3: (a) Dimensions and (b) displacement of the proposed device.

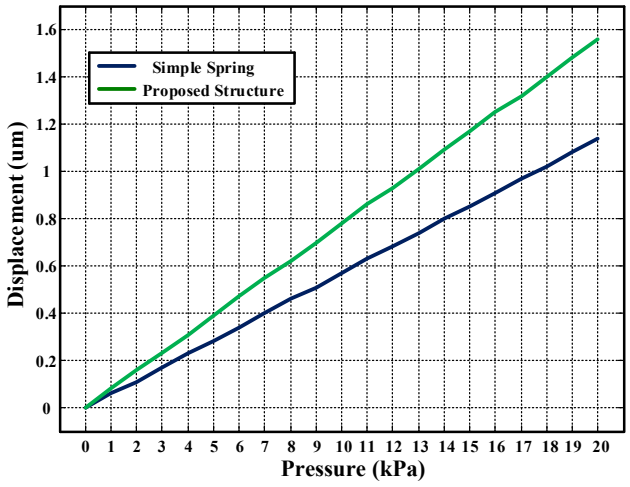

Figure 5: Displacement versus pressure in the range of 1–20 kPa.

Results and discussion

Analysis of spring stiffness coefficient

Among different parameters that affect the sensitivity of the sensor, one of the most important parameters is the spring stiffness coefficient, which determines the resistance of the diaphragm to the applied pressure. If this parameter is too low, it leads to loosening of the diaphragm and determines the self-actuating. With the slightest change in the pressure or a small impact on the sensor, a change is seen in capacitance and the incorrect information is transmitted to the operator. On the other hand, if the spring stiffness coefficient is too high, the diaphragm will be stronger and the capacitance changes will occur at very high pressures. Therefore, the necessary care must be taken in designing the spring so that is prevented from falling into these two extreme cases. Equations (3) and (4) show how to obtain the spring stiffness coefficient.

$$K = \frac{EWt^3}{L^3} \tag{3}$$

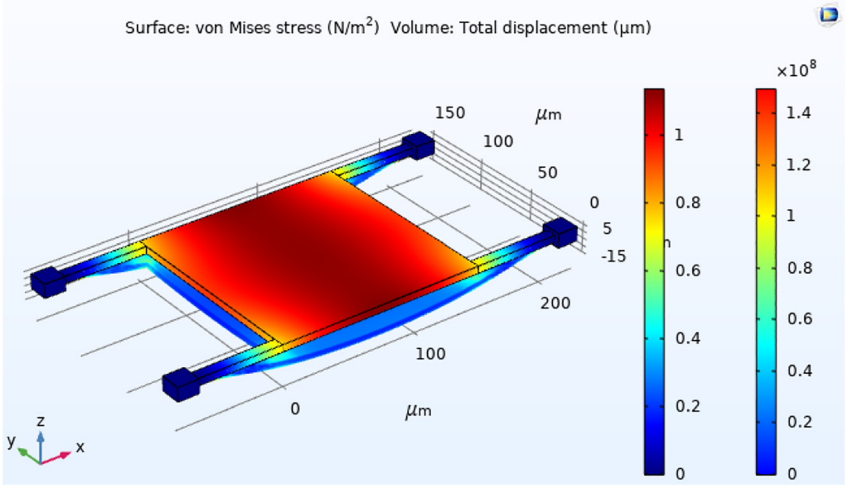

Figure 4: Displacement and stress profile of the device with the simple spring.

$$\frac{1}{K_B} = \frac{1}{K_1} + \frac{1}{K_2} + \frac{1}{K_3} + \cdots \quad (4)$$

where, K is the spring stiffness coefficient and E is the Young's modulus.

Using these equations, K_B for the springs was obtained 166 N/m. Given that there are four springs in the proposed sensor, K_B must be quadrupled.

Displacement and capacitance

According to Equations (3) and (4), the spring stiffness coefficient depends on the Young's modulus, the dimensions of each spring and the number of springs. By simulating the proposed sensor in COMSOL software, the amount of the displacement and the air gap at different pressures are obtained. Using equations (1) and (2), fixed capacitance and variable capacitance can also be calculated. Table 1 contains the simulation results.

The dielectric layer capacitance (C_1) will always be constant. The capacitance created in the air gap (C_2) will change with the amount of pressure, and the total capacitance is obtained from the sum of C_1 and C_2. For a better understanding, the variations of the total, fixed and variable capacitances with the pressure are shown in Figure 6.

As illustrated in Figure 6, the variations of the total capacitance follows that of the variable capacitance. As expected in higher pressures the total capacitance changes more. To understand the ratio of the capacitance change to the pressure change the sensitivity of the sensor has been calculated and discussed in the next section.

Sensitivity

The ratio of changes in the capacitance (output) to the applied pressure (input) will indicate the sensitivity. In fact, by having a greater change in the capacitance in response to lower applied pressure, a more sensitivity is obtained. Equation (5) is given to obtain the sensitivity.

$$S = \frac{\Delta C}{\Delta P} = \frac{C_2 - C_1}{P_2 - P_1} \quad (5)$$

where, C_1 and C_2 are the total capacitances for the two applied pressures in a row in Table 1. The calculated sensitivity for the proposed sensor can be seen in Table 2. As expected, as the pressure increases, the sensitivity increases due to the reduction of air gap at higher pressures. As mentioned before, C_1 is fixed, so according to Equation (5), the sensitivity will only depend on C_2. Table 2 is in correspondence to Figure 4 that shows the variations of C_2 versus the applied pressure. Due to the ascending slope of

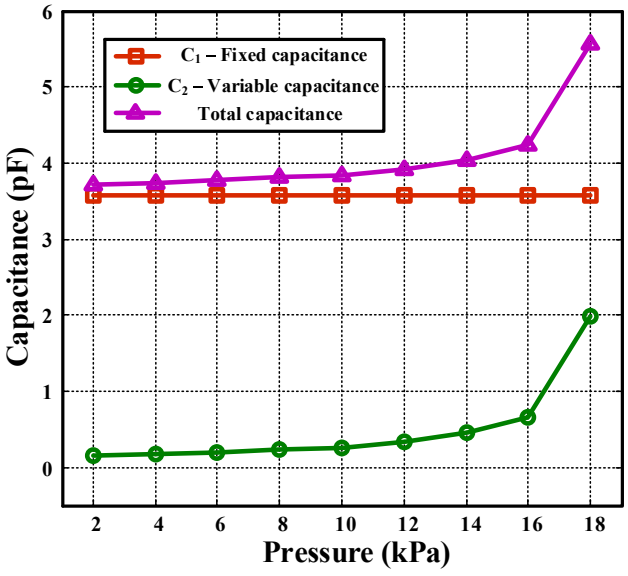

Figure 6: The total, fixed and variable capacitances versus pressure.

Table 1: The characteristics of the MIM capacitive pressure sensor.

Pressure (kPa)	Displacement (um)	Air gap (um)	C_1 (pF)	C_2 (pF)
2	0.14	1.36	3.58	0.146
4	0.3	1.2	3.58	0.165
6	0.45	1.05	3.58	0.189
8	0.65	0.85	3.58	0.234
10	0.7	0.8	3.58	0.248
12	0.9	0.6	3.58	0.331
14	1.07	0.43	3.58	0.463
16	1.2	0.3	3.58	0.663
18	1.4	0.1	3.58	1.99

Table 2: Sensitivity of the proposed MEMS sensor.

Pressure (kPa)	Sensitivity ($\times 10^{-3}$ pF/kPa)	
	Proposed structure	Simple spring
2	7	5.5
4	9.5	7
6	12	7
8	22.5	10
10	7	11.5
12	41.5	14
14	66	21
16	100	26.5
18	663	38.5

the curve, not only the variable capacitance itself increases, but also the capacitance change increases in higher pressures. According to Equation (5), this in turn, improves the sensitivity of the sensor in high pressures.

The sensitivity of the sensor has also improved compared to the structure with simple springs. The paper thus has reached its goals which were analysis and improvement of the sensitivity of capacitive MEMS pressure sensors.

Conclusions

A capacitive pressure sensor with four springs is designed. The spring design could successfully improve the displacement of the diaphragm and the sensitivity of the sensor. A square diaphragm with dimensions of 150 μm × 150 μm and a thickness of 5 μm has been used. By applying a maximum pressure of 20 kPa, the diaphragm is bent up to 1.5 μm touched the upper electrode. A very good linear response was obtained. The capacitance value and the sensitivity increased by applying pressure from 1 to 20 kPa. An improved sensitivity of 663 ($\times 10^{-3}$) (pF/kPa) was achieved at 18 kPa.

Author contributions: All the authors have accepted responsibility for the entire content of this submitted manuscript and approved submission.
Research funding: None declared.
Conflict of interest statement: The authors declare no conflicts of interest regarding this article.

References

Ansari, H. R., and M. B. Taghaddosi. 2020. "Optimization and Development of the RF MEMS Structures for Low Voltage, High Isolation and Low Stress." *Analog Integrated Circuits and Signal Processing* 101: 659–68.

Ansari, H. R., and Z. Kordrostami. 2020. "Development of a Low Stress RF MEMS Double-Cantilever Shunt Capacitive Switch." *Microsystem Technologies* 26: 2739–48.

Amiri, P., and Z. Kordrostami. 2018. "Sensitivity Enhancement of MEMS Diaphragm Hydrophones Using an Integrated Ring MOSFET Transducer." *IEEE Transactions on Ultrasonics, Ferroelectrics, and Frequency Control* 65: 2121–30.

Ansari, H. R., and S. Khosroabadi. 2018. "Low Actuation Voltage RF MEMS Shunt Capacitive Switch with High Capacitive Ratio." In *Iranian Conference on Electrical Engineering (ICEE)*.

Ansari, H. R., Z. Kordrostami, and S. Hamedi. 2020. "Effect of Passive Elements on the Isolation of a Pin-Pin RF MEMS Switch in an Electrical Circuit." In *Iranian Conference on Electrical Engineering (ICEE)*.

Ansari, H. R., and S. Khosroabadi. 2019. "Design and Simulation of a Novel RF MEMS Shunt Capacitive Switch with a Unique Spring for Ka-Band Application." *Microsystem Technologies* 25: 531–40.

Ghoddus, H., Z. Kordrostami, and P. Amiri. 2019. "Performance Enhancement of MEMS-Guided Four Beam Piezoelectric Transducers for Energy Harvesting and Acceleration Sensing." *International Journal of Modern Physics B* 33 (18).

Ghoddus, H., and Z. Kordrostami. 2018. "Harvesting the Ultimate Electrical Power from Mems Piezoelectric Vibration Energy Harvesters: an Optimization Approach." *IEEE Sensors Journal* 18: 8667–75.

Kordrostami, Z., and S. Roohizadegan. 2018. "A Groove Engineered Ultralow Frequency Piezomems Energy Harvester with Ultrahigh Output Voltage." *International Journal of Modern Physics B* 32 (20): 1850208.

Kordrostami, Z., and S. Roohizadegan. 2019. "Particle Swarm Approach to the Optimisation of Trenched Cantilever-Based MEMS Piezoelectric Energy Harvesters." *IET Science, Measurement & Technology* 13: 582–8.

Mafinejad, Y., A. Z. Kouzani, M. Nassabi, Y. Lim, and K. Mafinezhad. 2015. "Characterization and Optimization to Improve Uneven Surface on MEMS Bridge Fabrication." *Displays* 37: 54–61.

Mafinejad, Y., A. Kouzani, K. Mafinezhad, and R. Hosseinnezhad. 2017. "Low Insertion Loss and High Isolation Capacitive RF MEMS Switch with Low Pull-In Voltage." *International Journal of Advanced Manufacturing Technology* 93: 661–70.

Mafinejad, Y., H. R. Ansari, and S. Khosroabadi. 2020. "Development and Optimization of RF MEMS Switch." *Microsystem Technologies* 26: 1253–63.

Rebeiz, G. M. 2003. *RF MEMS: Theory, Design, and Technology*, 3rd ed. New Jersey: John Wiley & Sons.

Rao, K., B. Reddy, V. Teja, G. V. S. Krishnateja, P. Kumar, and K. Ramesh. 2020. "Design and Simulation of MEMS Based Capacitive Pressure Sensor for Harsh Environment." *Microsystem Technologies* 26: 1875–80.